Magnetic resonance imaging of primary malignant bone tumors

J.L. Bloem, M.D.,*

R.G. Bluemm, M.D.*#

A.H.M. Taminiau, M.D.†

A.T. van Oosterom, M.D.‡

J. Stolk, Ph.D.§

J. Doornbos, Ph.D.*

RadioGraphics index terms:
Skeletal radiology
MRI
Magnetic resonance imaging
musculoskeletal system
Radiation therapy
musculoskeletal system

Cumulative index terms:
Bone neoplasms,
MR studies
Magnetic resonance
(MR), comparative
studies

THIS EXHIBIT WAS DISPLAYED AT THE 71ST SCIENTIFIC ASSEMBLY AND ANNUAL MEETING OF THE RADIOLOGICAL SOCIETY OF NORTH AMERICA, NOVEMBER 17-22, 1985, CHICAGO, ILLINOIS. IT WAS RECOMMENDED BY THE MAGNETIC RESONANCE IMAGING PANEL AND WAS ACCEPTED FOR PUBLICATION AFTER PEER REVIEW ON SEPTEMBER 4, 1986.

From the Departments of Diagnostic Radiology (*), Orthopedic Surgery (†), and Clinical Oncology (‡), The University Hospital of Leiden, and the Department of Medical Statistics, State University of Leiden (§), Leiden, The Netherlands.

(#) Presently at the Department of Radiology, Academic City Hospital, Bielefeld, Federal Republic of Germany.

Supported in part by Grant IKW 8589 of the Netherlands Cancer Foundation.

Address reprint requests to J.L. Bloem, M.D., University Hospital of Leiden, Department of Radiology, Bld. 1, Mail area: C2-S, Rijnsburgerweg 10, 2333 AA Leiden, The Netherlands.

The authors find that MRI yields more useful information in a single study than CT, Tc scanning or angiography; they use it as the primary local staging procedure in malignant bone tumors.

Introduction

The purpose of this study is to determine the value of magnetic resonance imaging (MRI) in the management of patients with primary malignant bone tumors. What is the impact of MRI, in relation to other diagnostic procedures such as CT, on planning reconstructive limb saving surgery *(6,7,10-15)*?

Four topics will be discussed.

1. MRI characteristics
2. Staging
3. Monitoring chemotherapy
4. Future developments

Material and Methods

In 53 patients with primary malignant bone tumors, 80 MRI examinations were compared with 80 CT examinations (Table I). Twenty-four of these patients were prospectively evaluated; 29 were retrospectively evaluated. The CT and MRI examinations were analyzed independently and at random by two experienced radiologists. The tumors were staged for: 1. marrow involvement; 2. cortical destruction; 3. involvement of all muscle compartments in three different regions: the knee, the pelvis and shoulder (Table II); 4. involvement of the neurovascular bundle, and 5. involvement of joints.

MRI was compared with Tc bone scans in 24 patients and with angiography in 9 patients. The preoperative staging procedures were compared with gross specimens in 49 patients and with the histologic findings in all 53 patients. The specificity of MRI, based on morphology and MR characteristics, was tested in all patients. Monitoring of preoperative chemotherapy by MRI was evaluated in 8 patients.

MRI examinations were performed on a 0.15 T resistive (7 patients) or 0.5 T superconductive Philips[1] Gyroscan™ (46 patients). Spin echo (SE) pulse sequences with relative T1 weighting (TR 250-550, TE 30) and T2 weighting (TR 1000-2500, TE 50-100) were used. The intravenous administration of Gd-DTPA (0.1-0.2 mmol/kg body weight) was combined with fast field echo (FFE) in 8 patients. Slice thickness was 5-10 mm for surface and body coils *(8)*. CT scans were performed on several third and fourth generation scanners with scanning times of less than 4 seconds.

TABLE I
53 Patients 80 MRI Examinations

15 Osteosarcoma	2 Chordoma
19 Ewing sarcoma	1 Clear cell sarcoma
9 Chondrosarcoma	1 Giant cell tumor
3 Fibrosarcoma	1 Synovial sarcoma
2 Non-Hodgkin lymphoma	

TABLE II
Tumor location in 24 prospectively analysed patients

Knee	11
Pelvis	6
Shoulder	6
Toe	1

Results

MRI CHARACTERISTICS AND SIGNAL INTENSITY (s.i.)

• Osteosclerotic tumors (in particular sclerotic osteosarcomas) have a low s.i., which is independent of the pulse parameters used because of low spin density and short T2 relaxation time (Table III) *(2,4,5,16)*.

• Osteolytic tumors, in general, have a high s.i. on T2, and a low s.i. on T1 weighted images because of prolonged T1 and T2 relaxation times *(2,4,5,16)*.

• Telangiectatic osteosarcomas may have a high s.i. on T1 weighted images because of the large blood filled cavities *(1)*. They must be differentiated from massive bleeding in any other type of tumor and from aneurysmal bone cysts.

• Uncalcified cartilage may have a relatively high s.i. on T1 weighted images; this, in combination with the lobulated margin, permits a specific diagnosis to be made (Figure 1). Chondrosarcoma cannot, however, be differentiated from enchondroma.

TABLE III
Signal Intensity (s.i.) in 23 Patients
S.I. OF TUMOR RELATIVE TO S.I. OF BONE MARROW

T1 weighted images	High	Low
Osteolytic tumor	2	12
Sclerotic tumor	–	9
T2 weighted images	**High**	**Low**
Osteolytic tumor	14	–
Sclerotic tumor	–	9

[1]Philips Medical Systems Division, Eindhoven, The Netherlands.

• On T2 weighted images, the intraosseous s.i. of tumor is usually equal to the extraosseous s.i. of tumor, but it may occasionally (5 patients) be lower than the extraosseous s.i.

• No differences in relative s.i. were found among the various histologic types with the exception of the above mentioned sclerotic osteosarcomas, telangiectatic osteosarcomas and cartilage tumors (Figures 1 and 2).

1A

1B

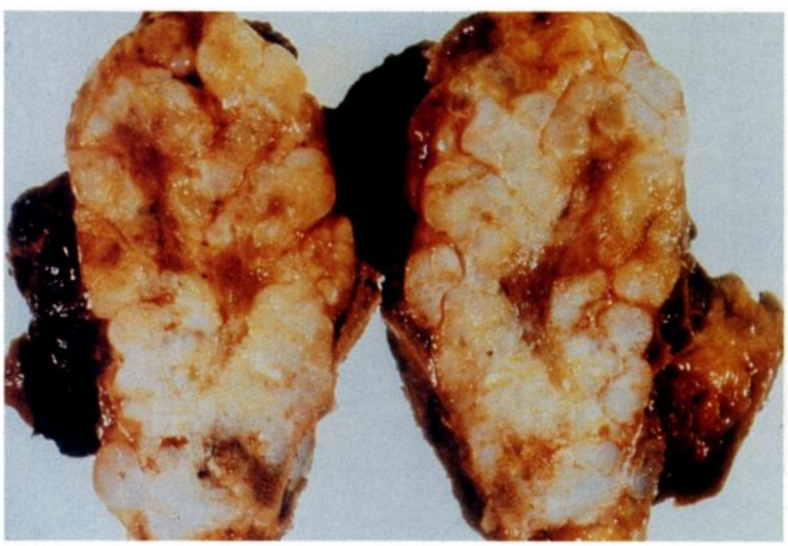

1C

Figure 1
Chondrosarcoma of the iliac bone (A) The typical lobulated appearance and high signal intensity are typical of the tumor. (Transverse plane; spin echo (SE) technique; TR 1600/TE 50) (B) Sagittal plane SE, TR 2700/TE 50 (C) Surgical specimen, cut in the sagittal plane, has the same lobulated appearance.

STAGING

• For the evaluation of cortical bone, the circumference of each bone was divided into four quadrants (Table IV). Invasion of cortex by tumor is best shown on T2 weighted images by a disruption of the black cortical line and by the replacement of cortex by the relatively high signal intensity of tumor (Figure 3). MRI is slightly more sensitive than CT (Table IV) because the signal intensity of osteosclerotic tumor is still a little greater than the signal intensity of normal cortex (Figure 2). The high attenuation of osteosclerotic tumor is often indistinguishable from that of cortex on CT.

TABLE IV

Cortical Destruction
n = 92 quadrants in 23 patients
Tumor = 54 quadrants
Normal = 38 quadrants

	False Negative	False Positive
CT	5	4
MRI	1	1

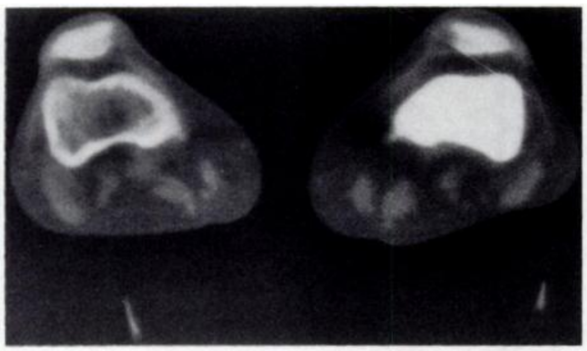

2A

2B

2C

Figure 2
Sclerotic osteosarcoma of the distal femur (A) CT cannot differentiate tumor from cortical bone; cortical involvement cannot be excluded. (B) The black line of normal cortex is easily differentiated from the inhomogeneous higher signal intensity of the osteosarcoma (Transverse plane, SE, TR 1800/TE 50). (C) (Sagittal plane, SE, TR 700/TE 30) On this more T1 weighted image, the difference between tumor and cortex is difficult to perceive. (D) The surgical specimen has been cut in the coronal plane; the cortex was not invaded by tumor.

2D

3A

3B

Figure 3
Chondrosarcoma of the femur (A) The high signal intensity of the tumor appears to invade the anterior cortex (arrow); no soft tissue extension is seen. (Sagittal plane, SE, TR 1500/TE 50) (B) The surgical specimen has been cut in the sagittal plane. Tumor invades the anterior cortex (arrow) but was confined to the bone.

• MRI is more accurate than CT in determining the extent of bone marrow involvement (Table V). This is because of superior contrast resolution on T1 weighted images in the ideal longitudinal (sagittal or coronal) plane (Figure 4). Although Tc bone scanning also displays bone marrow involvement in a longitudinal plane, it is less accurate than MRI (Table VI) because Tc scanning detects marrow disease indirectly, has poor spatial resolution, and shows increased uptake in areas of tumor-related hyperemia (Figures 4 and 5) *(1)*.

TABLE V
Intraosseous Tumor Length

Correlation Coefficients of CT and MRI by Pathologic Examination		
Knee (n = 11)	CT .920	MRI .998
Pelvis (n = 6)	CT .958	MRI .999
Shoulder (n = 6)	CT .953	MRI .993
Total (n = 23)	CT .950	MRI .997

4A

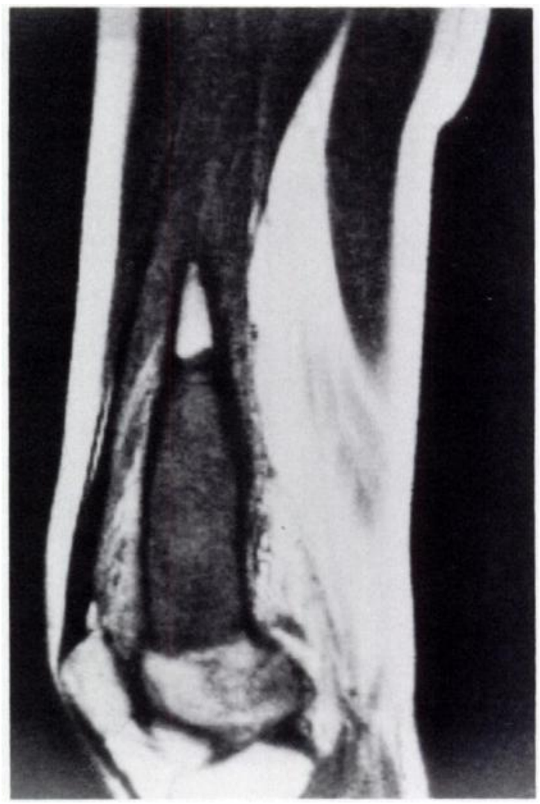

4B

4C

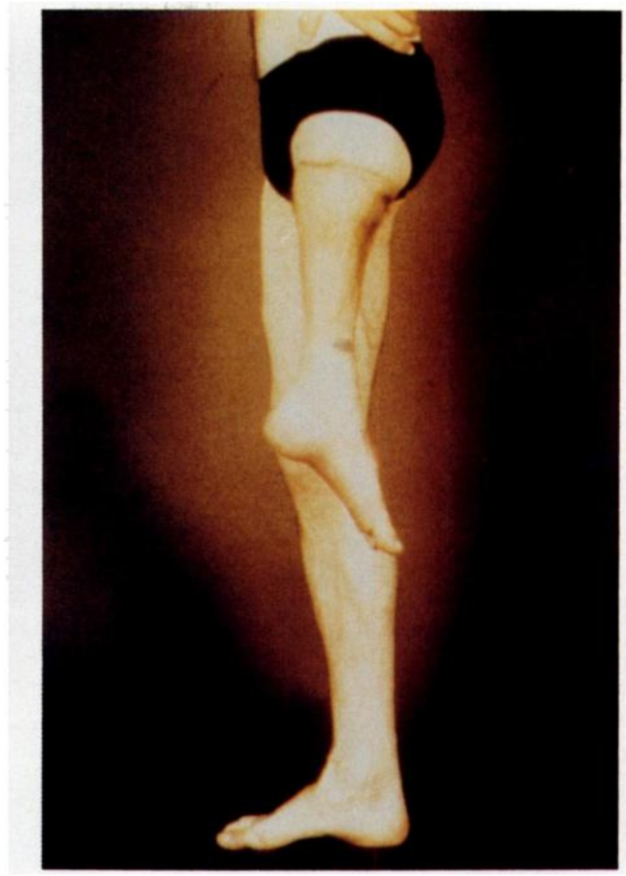

4D

Figure 4
Clear cell sarcoma (A) This anterior view of a Tc scan shows increased uptake of Tc-MDP in a clear cell sarcoma located in the distal femur. Accurate anatomic definition of tumor extent is difficult because normal bone accumulates almost no Tc-MDP. (B) In contrast to the Tc bone scan, this T1 weighted sagittal MR image clearly demonstrates the interface between tumor and normal marrow. (Sagittal plane; SE, TR 250/TE 30) (C) The neurovascular bundle is contiguous with the tumor; the joint is involved. (Sagittal plane SE, TR 1700/TE 50) (D) Treatment: excision of femur and rotation osteoplasty.

TABLE VI
Opinion of the Surgeon on Intraosseous Tumor extent

MRI superior to CT	12
MRI equal to CT	12
MRI inferior to CT	0
MRI superior to Tc-scan	10
MRI equal to Tc-scan	14
MRI inferior to Tc-scan	0

5A 5B 5C 5D

Figure 5
Fibrosarcoma (A) A CT scout view demonstrates bone destruction involving the femur and tibia in this patient with a fibrosarcoma of the femur. (B) This CT scan at the level of the femoral condyles shows tumor with cortical bone destruction. (C) This CT scan at the level of the tibia shows osteolysis which may be caused by tumor or tumor related hyperemic osteoporosis. (D) Sagittal, Gd-DTPA enhanced, T1 weighted image demonstrates tumor in the femur. The cruciate ligaments insert in the tumor. The tibia has normal signal intensity allowing a diagnosis of tumor related hyperemic osteoporosis to be made. The normal signal intensity of bone marrow in the tibia excludes the presence of tumor. Gd-DTPA was used because this patient could only tolerate a short examination time.

• Soft tissue extension in particular muscle compartments and soft tissue extension in relation to large vessels and joints are best shown on T2 weighted images in the transverse plane. Additional sagittal and sometimes coronal sections often increase sensitivity, however, especially in demonstrating the relationship of tumor to vascular structures (Figures 6 and 7). MRI is superior to CT in staging the soft tissue extension of tumor (Tables VII-XII) *(1,2,16)*. The value of MRI was not influenced by the anatomical location (knee, pelvis, shoulder).

6A

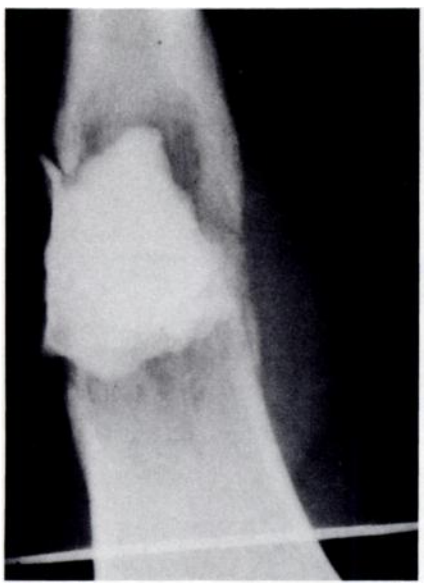

6B

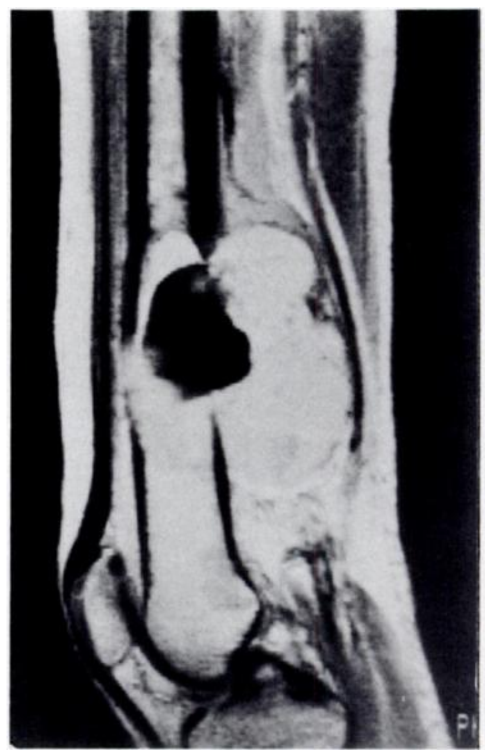

6C

Figure 6
Fibrosarcoma (A) The presence of intra- and extraosseous tumor and cortical destruction can be appreciated in this CT scan. Posterior soft tissue extension, however, is difficult to define. (B) This AP radiograph of the distal femur was exposed after biopsy, cement had been used to stop bleeding. (C) MR provides an accurate display of tumor extension into the adductor compartment. The femoral artery is displaced; the posterior and anterior cortices are invaded. Cement is seen as absence of signal. (Sagittal plane; SE, TR 1050/TE 50)

7A

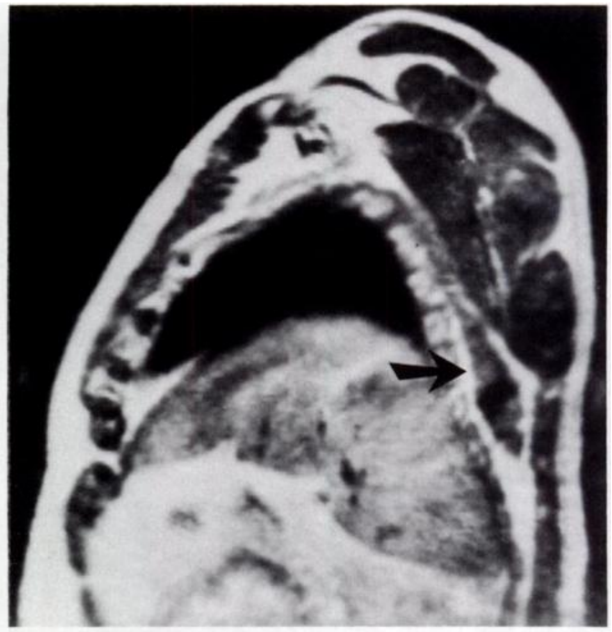

7C

Figure 7
Chondrosarcoma (A) A chondrosarcoma of the scapula, with calcifications, is visualized by CT. This CT section fails to show the relationship of the tumor to the teres major muscle. (B) On this MR image, the high signal intensity of the tumor infiltrating the infraspinatus muscle is easily perceived. (Transverse plane; SE, TR 1500/TE 50) (C) The teres major muscle (arrow) is seen to be normal in this sagittal MR image. (Sagittal plane; SE, TR 1000/TE 50)

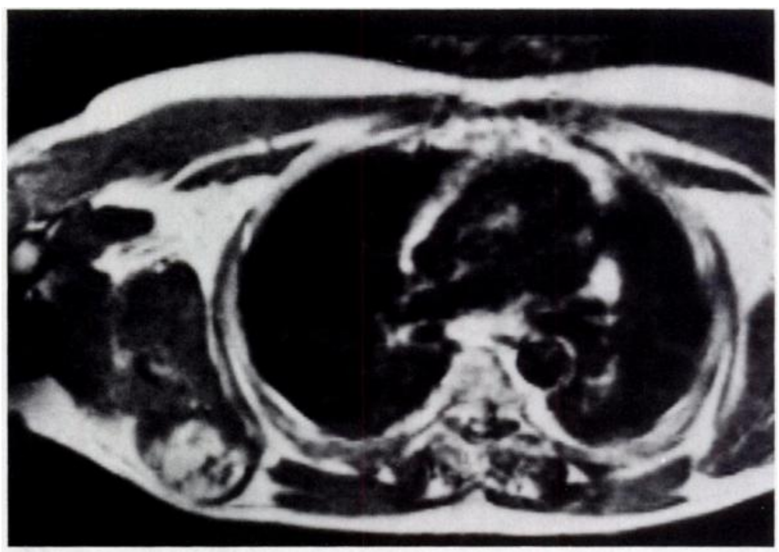

7B

TABLE VII
The Knee: Soft Tissue Extension

11 patients studied, 8 different compartments evaluated in each patient n = 88 compartments of which 20 were truly involved by tumor

	CT	MRI
False Positive	0	0
False Negative	4	0
True Positive	16	20
True Negative	68	68

TABLE VIII
Pelvis: Soft Tissue Extension

6 patients studied, 17 compartments evaluated in each patient n = 102 compartments of which 23 were truly involved by tumor

	CT	MRI
False Positive	4	0
False Negative	9	4
True Positive	14	19
True Negative	75	79

TABLE IX
Shoulder: Soft Tissue Extension

6 patients studied, 9 muscle compartments evaluated in each patient n = 54 muscle compartments of which 7 were truly involved by tumor

	CT	MRI
False Positive	3	1
False Negative	1	0
True Positive	6	7
True Negative	44	46

TABLE X
Opinion of the Surgeon on Soft Tissue Extension

n (number studied by CT and MRI) = 24	
MRI superior to CT	17
MRI equal to CT	7
MRI inferior to CT	0

TABLE XI
Vascular Involvement

n (number studied by CT, MRI and angiography) = 9		
n (number studied by CT and MRI) = 15		
False Positive:	CT/MRI/Angio	0
False Negative:	CT (Femoral A.)	1
	MRI/Angio	0
Positive at pathologic examination (Axillary artery, Femoral artery)		2

TABLE XII
Opinion of the Surgeon on Vascular Involvement

n (number studied by MRI and CT) = 24	
MRI superior to CT	10
MRI equal to CT	14
MRI inferior to CT	0
n (number studied by MRI and angiography) = 9	
MRI superior to angiography	5
MRI equal to angiography	3
MRI inferior to angiography	1
No angiography performed	15

Only one false positive and four false negative diagnoses were made on the basis of MR images. All four false negative diagnoses were made in one patient with a Ewing sarcoma of the femur (four different muscle compartments in the hip region). Following chemotherapy, the signal intensity of these four muscle compartments returned to normal. At histologic examination, however, tumor residue was found (Figure 8).

The relationship of tumor to large vessels is slightly better demonstrated on MRI than on CT (Tables XI and XII). Neither MRI nor CT nor angiography can reliably differentiate displacement of vessels by tumor from fixation in a given case of soft tissue invasion by tumor.

Angiography seldom provided information that was not available on MRI (Tables XI, XII, Figures 9 and 10).

Joint effusion and involvement are easily depicted by MRI. Involvement of articular surfaces, which are often parallel to the transverse CT plane is easier to evaluate by MRI than by CT (Figure 4).

8A

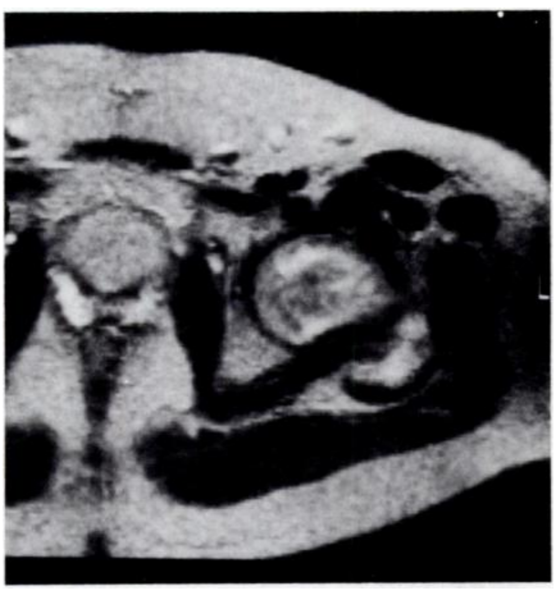

8B

8C

Figure 8
Ewing sarcoma after chemotherapy and irradiation (A) MRI and CT both failed to demonstrate involvement of the quadrate, piriformis, and inferior and superior gemelli muscles. Tumor infiltrated these muscles at their insertions on the femur. (Transverse plane; SE, TR 1350/TE 50) (B) At the same level, no abnormalities are seen on this more T2 weighted MR sequence. (Transverse plane; SE, TR 1350/TE 100) (C) In this MR scan below the trochanter, tumor is seen anterior to the femur.

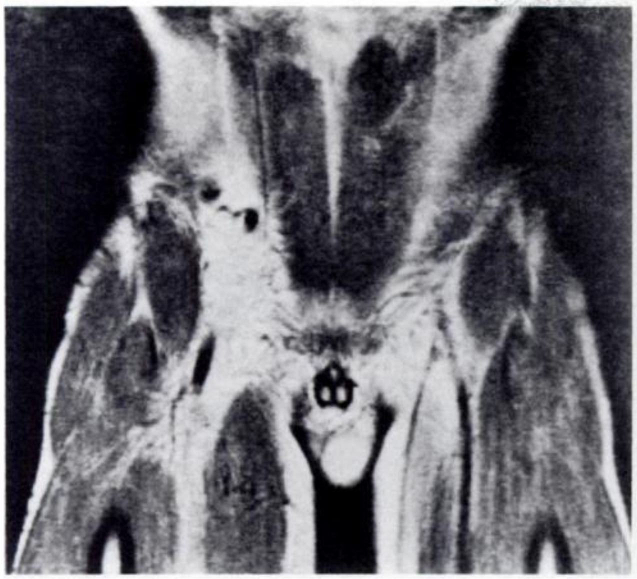

9A

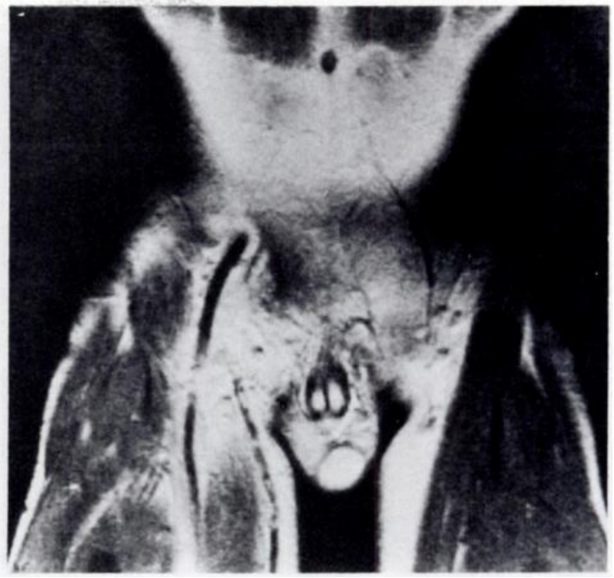

9B

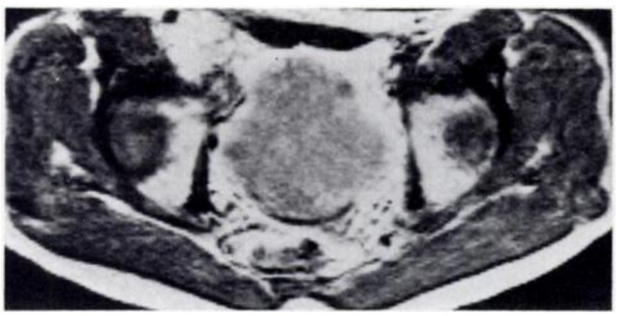

9C

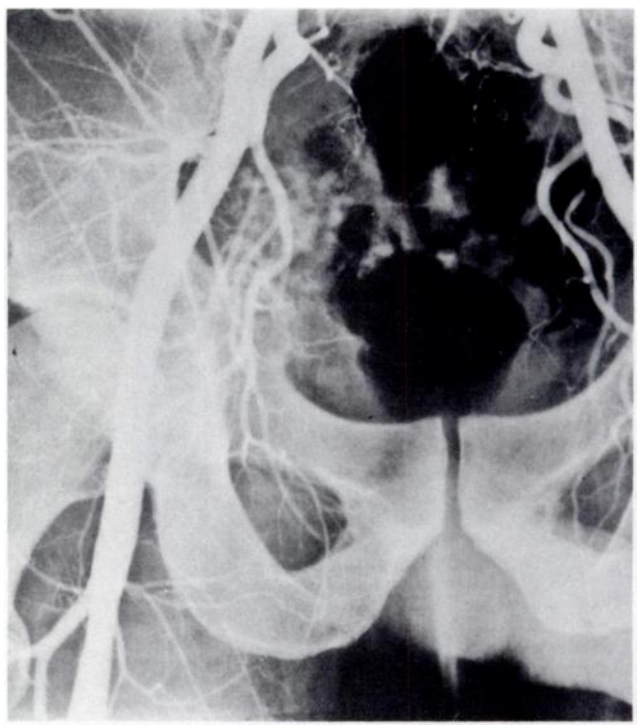

9D

Figure 9
Chondrosarcoma (A) At the level of the chondrosarcoma, the iliac artery is leaving the imaging plane. The femoral artery, inferior to the tumor is entering the imaging plane. (Coronal plane; SE, TR 1500/TE 50) (B) In this MR section made with the same pulse sequence, but 1 cm more anterior, the artery is better visualized. (C) The femoral artery is stretched over the lobulated chondrosarcoma, which arises from the pubic bone. The central calcified part has a low signal intensity, the noncalcified part has a high signal intensity. (D) Angiography provides no additional information. Tumor calcifications and the femoral artery, which is stretched over the tumor, are demonstrated.

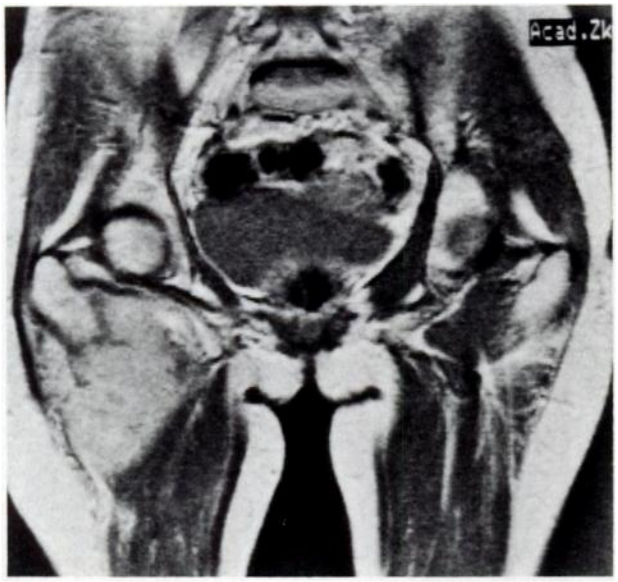

10A

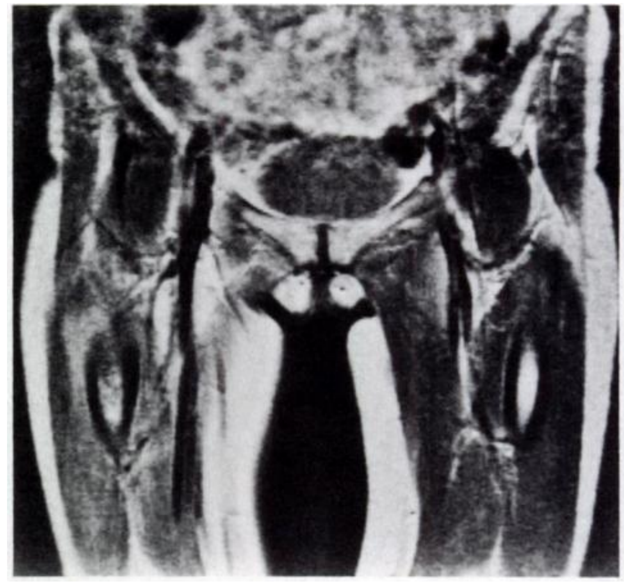

10B

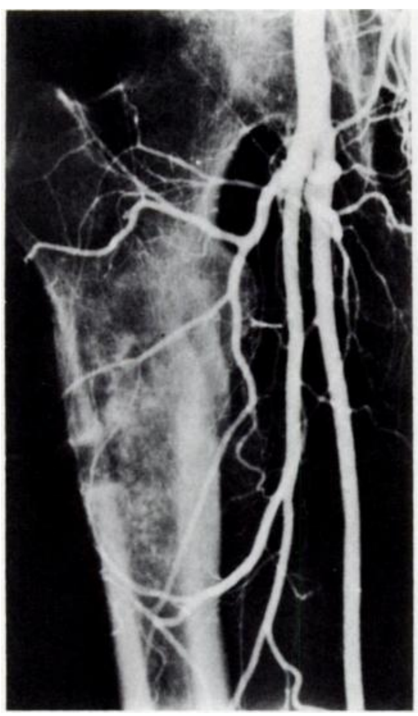

10C

10D

Figure 10
Chondrosarcoma (A) Chondrosarcoma of the proximal femur is clearly shown on a coronal MR image. (SE, TR 1500/TE 50) (B) More anteriorly, the superficial femoral artery is stretched over the tumor, whereas, the proximal part of the deep femoral artery is encased by tumor. (Coronal plane; SE, TR 1500/TE 50) (C) Angiography does not show displacement of the femoral arteries. (D) This is the surgical specimen, cut in the coronal plane.

CHEMOTHERAPY

MRI can indicate response to chemotherapy *(1,2)*. MRI findings that indicate a satisfactory response are (Figures 11 and 12): 1, decrease in tumor volume; 2, decrease of signal intensity on T2 weighted images (4 patients), which may be caused by dehydration of tumor, calcification or fibrosis; 3, marked increase of signal intensity (on T2 weighted sequences) owing to necrosis or hemorrhage (2 patients).

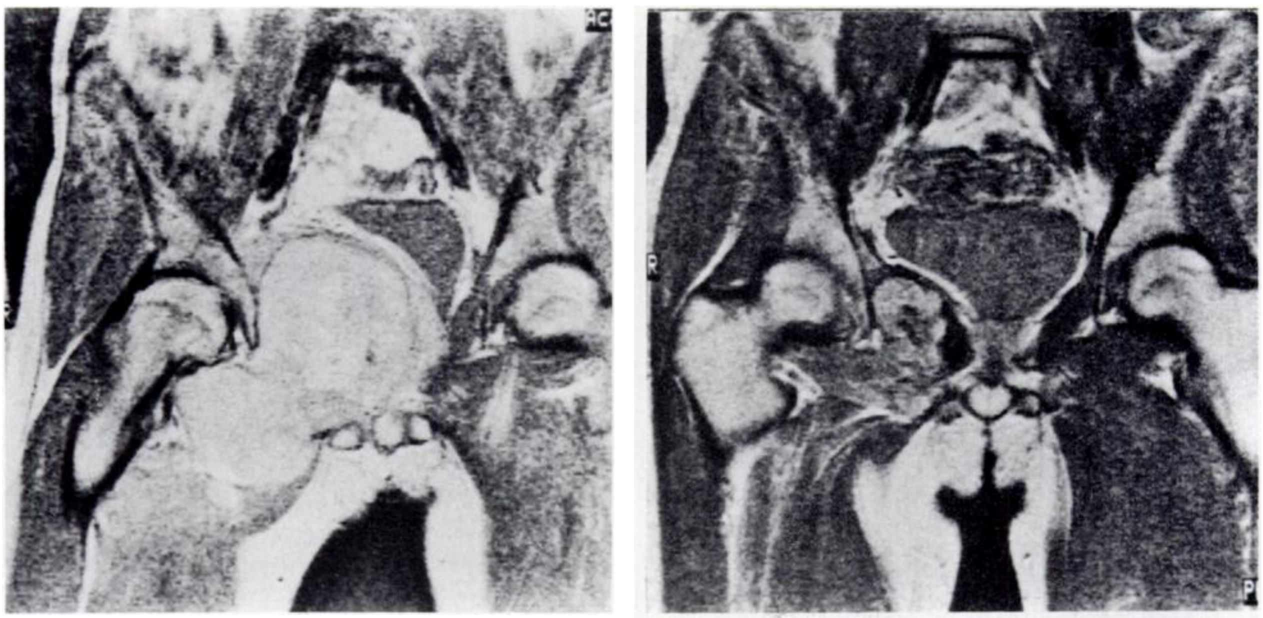

11A **11B**

Figure 11
Ewing sarcoma (A) A coronal view of a Ewing sarcoma originating in the right pubic bone. The huge tumor has a high signal intensity prior to chemotherapy. (SE, TR 1000, TE 50) (B) Following chemotherapy, the decrease in tumor volume and signal intensity indicate satisfactory response. (Coronal plane; SE, TR 1000, TE 50)

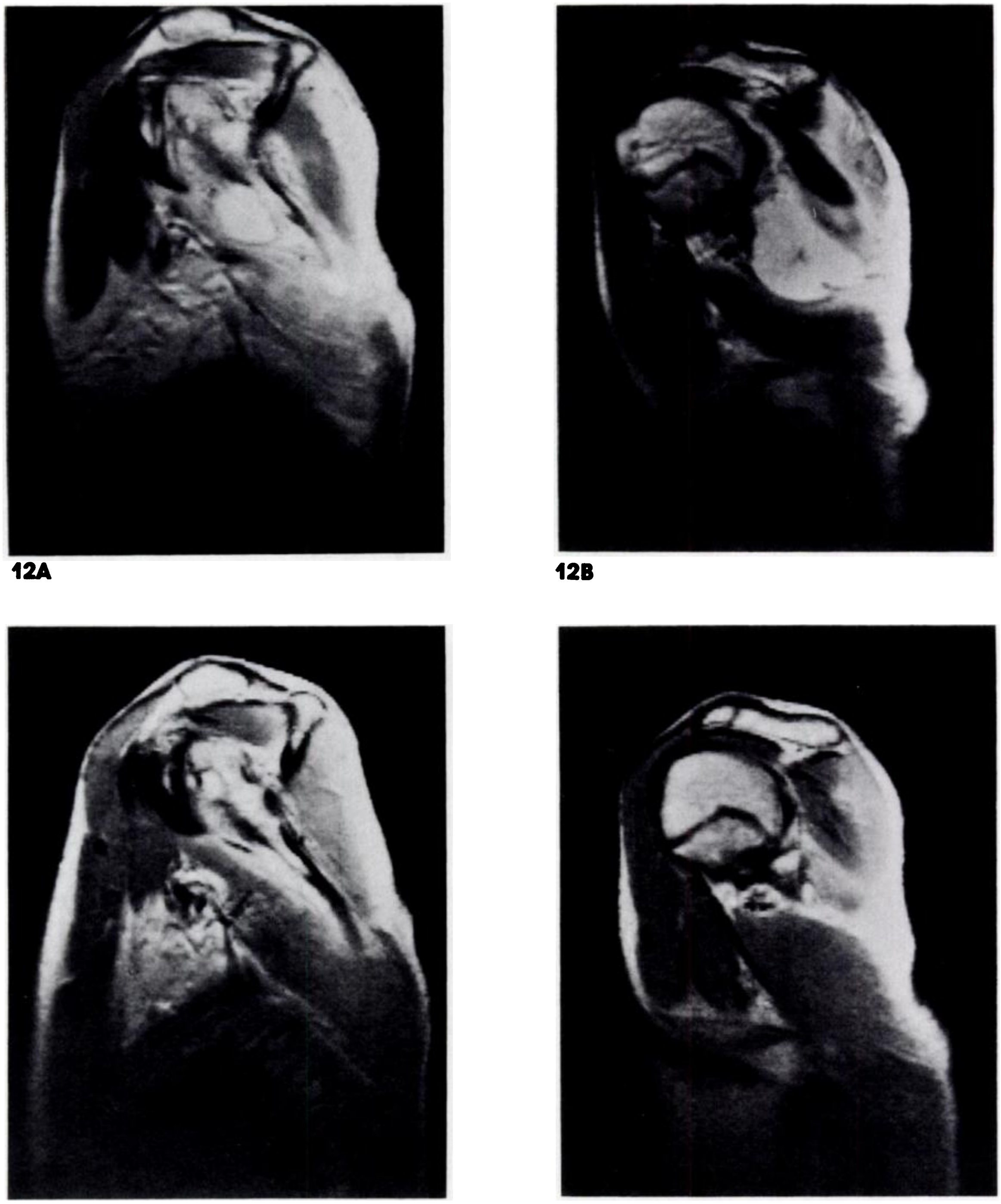

12A **12B** **12C** **12D**

Figure 12
Fibrosarcoma (A&B) Large fibrosarcoma in the axillary fossa prior to chemotherapy: the teres major muscle is displaced. (Sagittal TR 1950/TE 50, at the level of the scapula (A) and humerus (B)) (C&D) Satisfactory response following chemotherapy: the axillary fossa is now free of macroscopic tumor and only residual changes are seen. (Sagittal plane; SE, TR 1950/TE 50)

MRI findings that indicate an unsatisfactory response are (Figure 13): 1, stable signal intensity and tumor volume, or 2, increased tumor volume (2 patients).

13A

13B

13C

Figure 13
Osteosarcoma (A) This MR image shows the high signal intensity of an osteosarcoma of the femur with marked soft tissue extension, prior to chemotherapy. The large vessels are contiguous with the tumor. (Sagittal plane; SE, TR 1500/TE 50) (B) Following chemotherapy, the tumor volume and signal intensity are essentially unchanged. Their stability indicates a poor response to chemotherapy. Chemotherapy was discontinued, and an amputation was performed. (Sagittal plane; SE, TR 1500/TE 50) (C) This transverse cut section of the surgical specimen shows sclerotic tumor; the vessels are contiguous with tumor (arrow).

NEW DEVELOPMENTS

Fast field echo (FFE) technique is ideal for studying enhancement patterns after the intravenous injection of Gd-DTPA because of its short acquisition time *(3)*. Gd-DTPA enhances viable tumor, resulting in a high signal intensity on T1 weighted images. This is caused by a shortened T1 relaxation time *(9)*. A 40-180% increase in signal intensity relative to the signal intensity of unenhanced T1 weighted images was observed. Gd-DTPA accumulates to a lesser degree in perifocal edema and nonviable tumor tissue (Figure 14). Enhancement patterns of certain histologic tumor types seem to increase specificity: Cartilage containing tumor components, for instance, enhance to a lesser degree than bone forming tumor components (Figure 15).

Because Gd-DTPA shortens T1 relaxation times, it can display viable tumor with high signal intensity relative to normal tissue such as normal muscle, with short T1 weighted pulse sequences. Gd-DTPA may, thus, shorten the examination time (Figure 16).

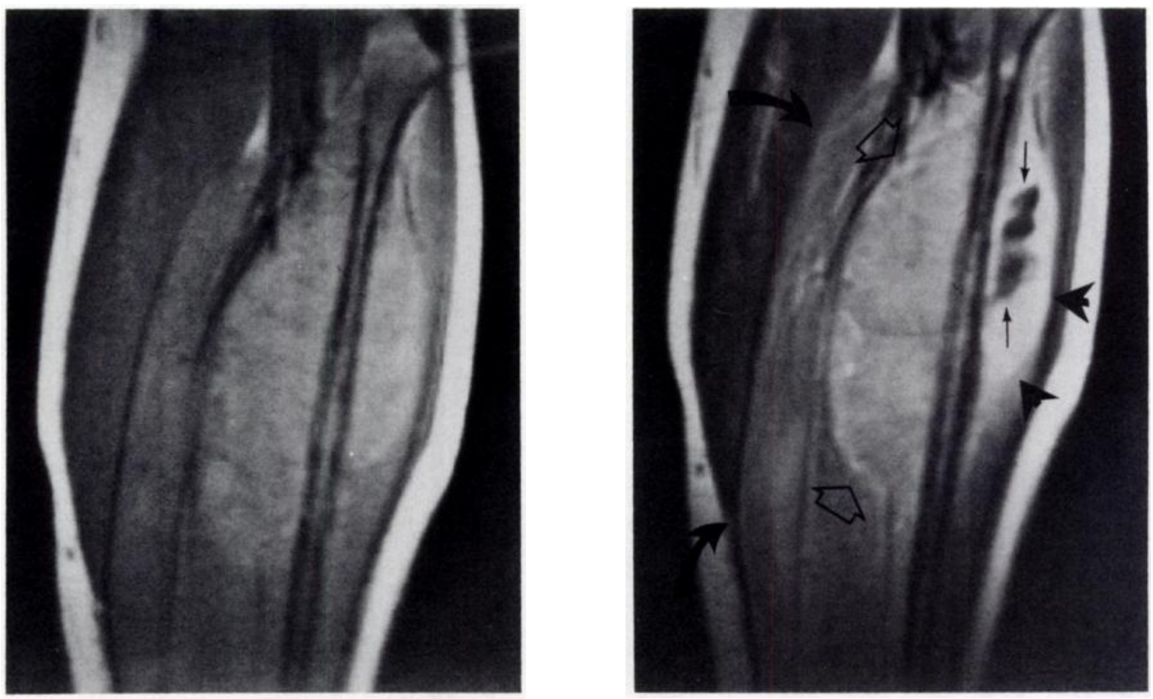

14A **14B**

Figure 14
Ewing Sarcoma (A) In this MR section made prior to the injection of Gd-DTPA, it is difficult to separate the viable part of this Ewing sarcoma from hemorrhage. (Coronal plane, SE, TR 550/TE 30) (B) After the injection of Gd-DTPA (TR 550/TE 30), strong enhancement of the tumor (arrowheads) relative to central hemorrhage (open arrows), necrosis (small arrows) and edema (curved arrows) is observed. This allows demarcation of viable tumor lateral to the fibula for biopsy.

15A

15B

Figure 15
Osteosarcoma (A) No tissue differentiation is seen within this large osteosarcoma of the pelvis. (Coronal plane; SE, TR 550/TE 30; matrix size 128 × 128) (B) This MR image made within one minute after Gd-DTPA injection and using the same pulse sequence as in (A), allows tissue differentiation. The central cartilage containing part of the lesion does not enhance, whereas, the osteoid forming part in the periphery of this osteosarcoma does enhance. The central unenhanced part of the tumor could be mistaken for necrosis.

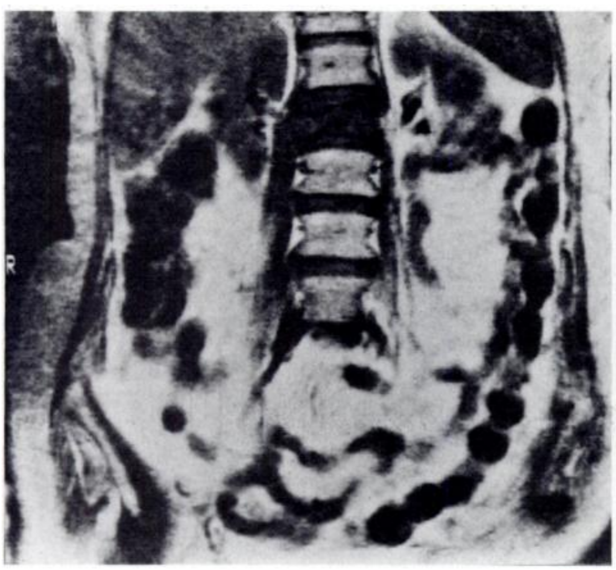

16A

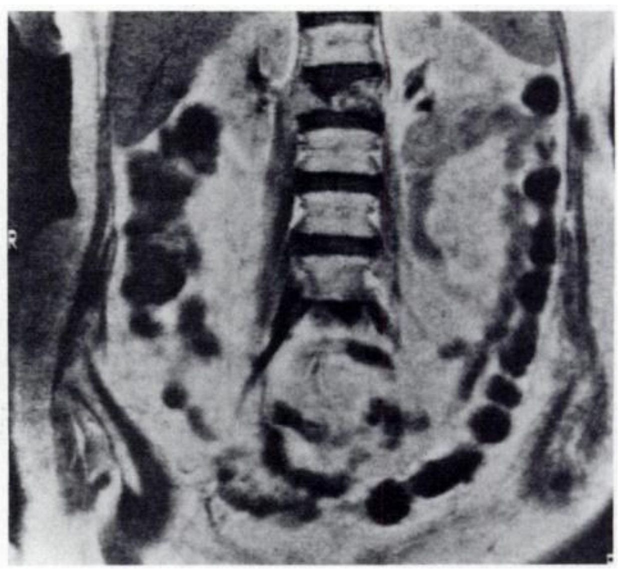

16B

Figure 16
Non-Hodgkin Lymphoma (A) This MR section clearly shows a non-Hodgkin lymphoma of low signal intensity in the second lumbar vertebra. (Coronal plane; SE, TR 550/TE 30) (B) Beacuse of severe pain, the patient could only tolerate a short examination, therefore, a short (SE, TR 550/TE 30) Gd-DTPA enhanced pulse sequence was used. Strong enhancement of the tumor results. Invasion into the right psoas muscle and pathological fracture are now clearly demonstrated.

Conclusions

• When T1 weighted images are used, MRI is significantly better than CT for staging intramedullary extension.

• Hyperemic osteoporosis can be differentiated from intramedullary tumor extension only by MRI; they cannot be distinguished with CT or Tc bone scanning,

• Although statistical proof is not yet available, results so far indicate that in staging soft tissue extension, MRI is better than CT.

• Cortical involvement can be accurately shown with T2 weighted images.

• Angiography seldom produces additional information not available with MRI alone.

• Cartilage, sclerotic and telangiectatic osteosarcoma: each often has a typical MRI appearance.

• The orthopedist's level of confidence is increased by MRI, and MRI may, thus, influence therapy planning (Table XIII).

• MRI can monitor chemotherapy. Signal intensity changes seem to precede changes in volume.

• Enhancement after Gd-DTPA administration increases tissue differentiation and shortens examination time.

In our hospital, MRI is used routinely as the *primary* local staging procedure, because it produces more useful information in one single study than CT, Tc bone scanning or angiography.

TABLE XIII
Impact on Therapy

n=24	
MRI superior to CT	12
MRI equal to CT	12
MRI inferior to CT	0
n=9	
MRI superior to angiography	9
MRI equal to angiography	0
MRI inferior to angiography	0
n=24	
MRI superior to Tc-scan	13
MRI equal to Tc-scan	11
MRI inferior to Tc-scan	0

References

1. Bloem JL, Falke THM, Tamlniau AHM, Van Oosterom AT, Steiner RM, Overbosch EH, Ziedses des Plantes Jr B. Magnetic resonance imaging of primary malignant bone tumors. RadioGraphics 1985; 5(6):853-886.
2. Bloem JL, Falke THM, Taminiau AHM, Van Oosterom AT, Doornbos J. Magnetic resonance imaging of primary malignant bone tumors. In: Magnetic resonance imaging and spectroscopy. M.A. Hopf, G.M. Bydder, eds. Proceedings First Congress of the European Society of Magnetic Resonance in Medicine and Biology. Rotoprint S.A., Carouge, Geneva, 1985:208-218.
3. Bluemm RG, Bloem JL, Doornbos J, Claus W, Taminiau AHM, Van Oosterom AT. Gadolinium DTPA-enhanced MR imaging of malignant bone tumors: Initial experience (WIP). Radiology 1985; 157(P):341.
4. Brady TJ, Gebhardt MC, Pykett IL, et al. Imaging of forearms in healthy volunteers and patients with giant cell tumor of bone. Radiology 1982; 144:549-552.
5. Brady TJ, Rosen BR, Pykett IL, McGuire MH, Mankin HJ, Rosenthal DI. NMR imaging of leg tumors. Radiology 1983; 149:181-187.
6. Campbell CJ. Place of resection in the management of primary bone tumors. Can J Surg 1977; 6:518-521.
7. DeSantos LA, Goldstein HM, Murray JA, Wallace S. Computed tomography in the evaluation of musculoskeletal neoplasms. Radiology 1979; 131:431-437.
8. Doornbos J, Grimbergen HAA, Booijen PE, Te Strake L, Bloem JL, Vielvoye GJ, Boskamp E. Application of anatomically shaped surface coils in MRI at 0.5 T. Mag Res in Med 1986; 3:270-281.
9. Felix R, Schoerner W, Laniado M, Niendorf H, Claussen C, Fiegler W, Speck U. Brain tumors: MR imaging with Gadolinium-DTPA. Radiology 1985; 157(P):125.
10. Forner JG, Kim DK, Shin MH. Limb preserving vascular surgery for malignant tumors of the lower extremity. Arch Surg 1977; 112:391-394.
11. Levine E, Lee KR, Neff JR, Maklad NF, Robeson RG, Preston DF. Comparison of computed tomography and other imaging modalities in the evaluation of musculoskeletal tumors. Radiology 1979; 131:431-437.
12. Lukens JA, McLeon RA, Sim FH. Computed tomographic evaluation of primary osseous malignant neoplasm. AJR 1982; 139:45-48.
13. Miller TR. Surgical management of malignant bone tumors. Can J Surg 1977; 20:513-517.
14. Morton DL, Eilber FR, Townsend CM, Grant TT, Mirra J, Weisdenburger TH. Limb salvage from a multidisciplinary treatment approach for the skeletal and soft tissue sarcomas of the extremity. Ann Surg 1976; 184:268-278.
15. Simon MA, Enneking WF. The management of soft tissue sarcomas of the extremities. J Bone Joint Surg (Am) 1976; 58:317-327.
16. Zimmer WD, Berquist TH, McLeod RA, et al. Bone tumors: Magnetic resonance imaging versus computed tomography. Radiology 1985; 155:709-718.

The authors thank W. van der Eyken, M.D., L. Papapoulou, M.D., S. de Lange, M.D. for their cooperation, and Mrs. F.H. Noorderijk and the Photographic Department for their assistance. Gd-DTPA was supplied by Schering-AG, Berlin, F.R.G.